Diffusion and following isothermal desorption of impurity and matrix atoms out of sapphire and its melt

N.P.Katrich, A.T.Budnikov, S.I.Krivonogov, Yu.P.Miroshnikov

Institute for Single Crystals, STC "Institute for Single Crystals",
National Academy of Sciences of Ukraine,
60 Lenin Ave., 61001 Kharkiv, Ukraine

Isothermal desorption of impurity and matrix atoms (as CO, CO_2, H_2, H_2O) out of sapphire bulk has been studied. A theoretical model has been proposed for diffusion mechanism of the atoms included in gas-vacancy complexes $2V^i$–M^i (M^i being an atom, V^i, a neutral vacancy). According to the model, the gas-vacancy complexes are formed due to breaking of ion-covalent bonds in sapphire. The impurity and matrix atoms that are diffused to the surface as components of the complexes are transformed into adsorbed state, then a fraction thereof becomes desorbed while another one becomes recombined into molecules and then desorbed. The equations describing the diffusion and desorption have been derived. The diffusion and desorption parameters have been determined for the atoms and molecules.

Исследована изотермическая десорбция примесных и матричных атомов из объема сапфира в составе CO, CO_2, H_2, H_2O. Предложена теоретическая модель механизма диффузии атомов в сапфире в составе газ-вакансионных комплексов $2V^i$–M^i (M^i — атом, V^i — нейтральная вакансия). Согласно модели газ-вакансионные комплексы образуются в результате разрыва ионно-ковалентных связей в сапфире. Примесные и матричные атомы, продиффундировав к поверхности в составе комплексов, переходят в адсорбированное состояние, затем одна часть их десорбируется, другая рекомбинирует в молекулы, после чего десорбируется. Получены уравнения, описывающие диффузию и десорбцию, определены параметры диффузии и десорбции атомов и молекул.

In sapphire single crystals grown in gas media by the melt horizontal crystallization in molybdenum crucibles, microparticles of unestablished composition may be formed along with gas pockets of $2 \cdot 10^{-4}$ to $4 \cdot 10^{-2}$ cm^3 size. The microparticles have a size less than 1 μm and the number may attain 10^6 to 10^8 cm^{-3}, depending on the pressure and composition of the gaseous medium where the crystallization occurs. In contrast to the gas pockets filled with carbon monoxide and hydrogen that are formed under the melt concentration overcooling in the intercellular hollows at the interface [1–3], the microparticles are formed at the smooth phase interface, too. Also, in contrast to the gas pockets, the microparticle formation is independent of the raw material purity. These experimental results form a base for assumption that the microparticles are formed either due to the melt deviation from stoichiometry, that is, to the melt (or crystal) supersaturation in certain products of Al_2O_3 dissociation, or due to the impurity metal oxides that attain the melt surface during the crystallization. Such oxides may be, in first turn, tungsten (molybdenum) oxides appearing due to interaction of oxygen being released from the melt (or crystal) with the crucible or heat shield materials of the growth chamber assembly. The
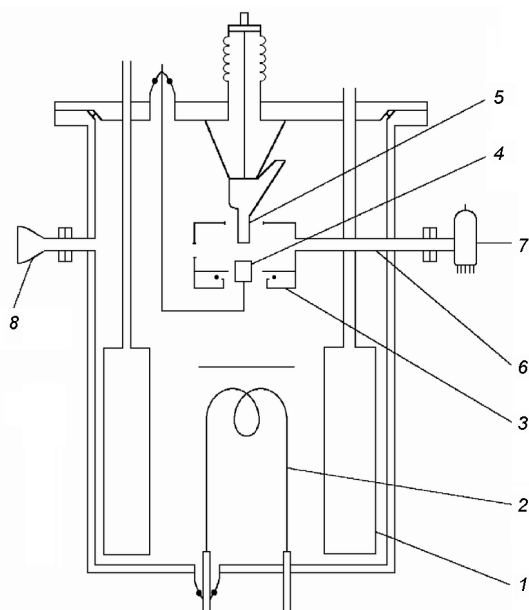
Fig. 1. Experimental unit chamber. *1*, liquid nitrogen vessel; *2*, titanium-molybdenum wire; *3*, circular electron gun; *4*, crucible; *5*, sampler; *6*, connecting nipple; *7*, RMO omegatron sensor; *8*, window.

inert gas medium seems to provide conditions for the melt deviation from stoichiometry and contamination. Since the crystal and its melt deviation from stoichiometry is defined by the impurity and matrix atoms release therefrom, the investigation of those processes are of great importance to establish the nature of the gas pockets and microparticles. We have already described some results of those studies [1–5]. The experimental data, however, were considered theoretically at a level insufficient to understand the mechanism of gas diffusion and desorption out of sapphire.

In our experiments, an ultrahigh vacuum unit was used including a chamber shown in Fig. 1. The chamber has been made of stainless steel with copper-sealed flanges, the gaskets allowing the chamber heating up to 700 K for degassing. The chamber contains a low-temperature pump made of titanium and consisting of a vessel *1* for liquid nitrogen and a titanium atomizer from titanium-molybdenum wire *2*; a circular electron gun *3*; a crucible *4* made of titanium single crystal; and a sampler *5* to feed the crucible with spherical samples of single-crystalline sapphire of 3.6 to 4 mm in diameter. The measuring chamber is defined by the electron gun case cooled with running water and connected by a nipple *6* to two omegatron sensors for gas partial pressure meas-
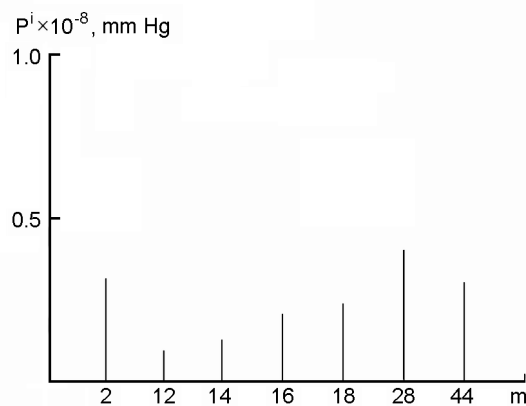

Fig. 2. Spectrum of gases in the analyzing chamber after the crucible degassing.

urements. The measuring chamber was pumped-off through holes of less than 10 cm^2 total area connecting it with the low-temperature titanium pump. The gases released from the sapphire and its melt were recorded using a RMO sensor and a IPDO-2 partial pressure gauge. The gas release rate was calculated as

$$\frac{d n^i}{dt} = (P^i - P^i_0) n^i_0 w^i, \qquad (1)$$

where P^i, P^i_0 are the partial pressures (mm Hg) of gases being desorbed out of sapphire inside and outside the measuring chamber, respectively; n^i_0, the number of particles in 1 cm^3 of a gas at $P = 1$ mm Hg and $T = 300$ K; w^i, the gas pumping-off rate that is defined by the flow capacity of the holes in the measuring chamber, cm^3/s. The isothermal gas desorption was studied using the following procedure. The sampler was loaded with spherical sapphire sampler. Then the chamber was pumped-off using a diffusion pump provided with water and nitrogen traps down to 10^{-6} mm Hg under simultaneous heating at 600 K for 3–4 h. After the chamber wall degassing, the vessel *1* was loaded with liquid nitrogen and the titanium vaporizer *2* was switched-on. The spongy titanium film formed at the vessel walls provided at 78 K absorption of all gases except for inert ones. The hydrogen pumping-off rate was about 10^7 cm^3/s. The residual gas pressure in the measuring chamber was lowered down to about 10^{-10} mm Hg. Then the electron gun was switched-on and the crucible was degassed under slow temperature elevation. The degassing was over at $T = 2800$ K. The temperature was measured by a tung-
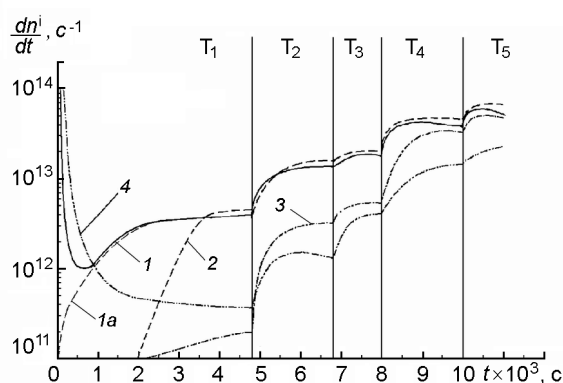
Fig. 3. Time dependence of isothermal desorption rate for CO (*1*), O_2 (*2*), CO_2 (*3*), H_2 (*4*). $T_1 = 1480$ K, $T_2 = 1650$ K, $T_3 = 1700$ K, $T_4 = 1990$ K, $T_5 = 2120$ K. The calculated curve for CO is also shown (*1a*).

sten-rhenium thermocouple and by an optical pyrometer (the shutter of window *8* was opened periodically using a magnet). The spectral composition of the gases after the crucible was degassed is shown in Fig. 2. After degassing, the crucible temperature was lowered to the preset value and a sapphire sample was dropped to the crucible using the sampler.

Fig. 3 presents the isothermal gas desorption out of sapphire. At $T = 1380$ K, the isothermal desorption rate of CO increases sharply in the moment when the sample drops into the crucible (curve 1) and then decreases to a minimum, then increasing slowly up to a value close to the maximum. An appreciable release of oxygen (curve 2) starts after an interval of about $2 \cdot 10^3$ s. The oxygen release rate increases from zero to a value close to the maximum within time interval $0 < t < 4.8 \cdot 10^3$ s, the maximum exceeding considerably the evaporation rate of oxygen being the Al_2O_3 dissociation product at the sapphire surface. Since neither oxygen atoms nor other ones are dissolved in interstitials of the sapphire hcp crystal lattice, it is just the matrix oxygen that is released from sapphire. After an about $2.4 \cdot 10^3$ s long pause, CO_2 release starts (curve 3). The initial rate of the CO isothermal desorption and the pause duration up to start of O_2 and CO_2 desorption have been found to depend on the surface purity of the sapphire sample. Thus, the initial section of the curve 1 is defined by CO desorption that is not connected with the release of carbon atoms out of the sapphire bulk. It is defined by desorption
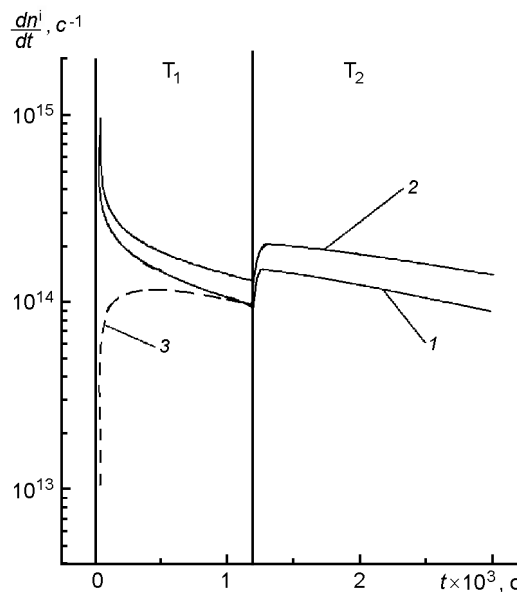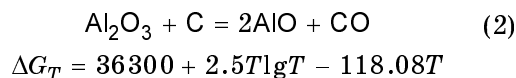

Fig. 4. Time dependence of isothermal desorption rate for CO (*1*) and CO_2 (*2*). $T_1 = 2250$ K, $T_2 = 2300$ K. The calculated curve for CO is also shown (*3*).

either of CO adsorbed from atmosphere or of CO formed at the sapphire surface as a result of chemical reactions, e.g.,

$$Al_2O_3 + C = 2AlO + CO \qquad (2)$$
$$\Delta G_T = 36300 + 2.5TlgT - 118.08T$$

between Al_2O_3 and carbon present as an impurity at the surface due to diamond grinding of the samples. The pauses in O_2 and CO_2 desorption can be explained by the fact that oxygen atoms diffusing out of the bulk are consumed to eliminate the oxygen deficiency in the sapphire surface layer ($2AlO + O = Al_2O_3$) that results from the reaction (2). The increased desorption rates of CO, CO_2 and O_2 in the interval $10^3 < t \le 4.8 \cdot 10^3$ s is defined mainly by diffusion of carbon and matrix oxygen atoms out of the bulk to the surface followed by the recombination thereof into CO, CO_2 and O_2 molecules. It is seen from Fig. 3 that every next jump-like elevation of the sapphire temperature results in increased isothermal desorption rates of the gases while the time intervals required to attain the maximum desorption rates are shortened. Similar results were obtained when studying the isothermal desorption of gases out of aluminum-yttrium garnet [3].

During the heating, some sapphire samples are subjected to failure that is accompanied by a sharp and relatively short-timed
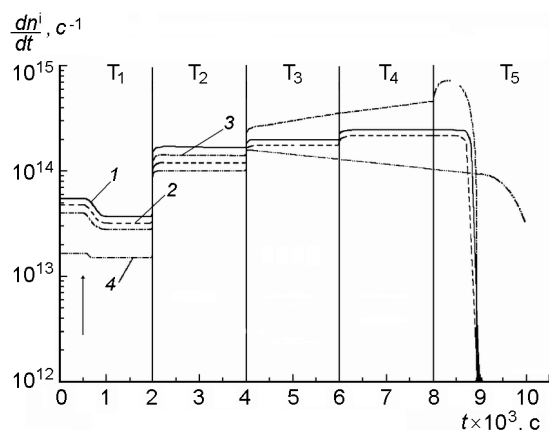
Fig. 5. Time dependence of evaporation rate out of Al_2O_3 melt for CO_2 (*1*), CO (*2*), O_2 (*3*), H_2 (*4*). $T_1 = 2320$ K, $T_2 = 2500$ K, $T_3 = 2540$ K, $T_4 = 2570$ K, $T_5 = 2630$ K. The onset of sapphire melting is indicated by arrow.

increase of the CO desorption rate [3]. When the sapphire temperature is increased from room to pre-melting one (2000 K and higher), then, in contrast to the case of $T = 1380$ K, not only CO and H_2 desorption rates but also that of CO_2 increase jump-like in the initial time period (Fig. 4). The desorption rates of the gases are lowered appreciably as the sapphire is melted, perhaps due to reduction of the free surface of the melted sample (Fig. 5). As the melt temperature is elevated step-by-step, those rates increase stepwise. At $T = 2540$ K, the isothermal desorption rate of oxygen increases in time (curve *2*). The melt seems to "boil" visually, the "boiling" is accompanied by pulsations of CO and CO_2 partial pressures, while those of hydrogen and oxygen do not pulse. The melt "boiling" and CO and CO_2 partial pressure pulsations can be assumed to be connected with destruction of gas bubbles filled with the gases emerging to the melt surface. At lower temperatures, the CO and CO_2 molecules seem to form clusters suspended in the melt, that is why the melt does not "boil" and the partial pressured do not pulse. At the final evaporation stage, the isothermal desorption rates drop to zero relatively fast. The hydrogen release after the melt evaporation (curve *4*) is explained by its release out of the crucible where it was dissolved during the melt evaporation.

Using the graphical integration of areas under dn/dt vs. t curves (Fig. 5), concentrations of carbon and hydrogen atoms in sapphire have been determined to be $C^C = (2.2$ to $2.4) \cdot 10^{19}$ cm^{-3} and $C^H = (1.8$ to $2) \cdot 10^{19}$ cm^{-3},
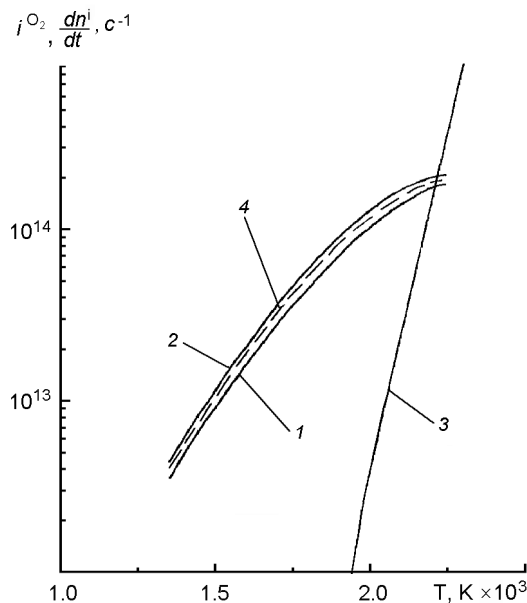

Fig. 6. Temperature dependences of isothermal desorption maximum rates for CO (*1*) and O_2 (*2*) and the O_2 evaporation rate (*3*). The calculated curve for CO is also shown (*4*).

respectively. The $dn^i/dt(T)$ dependences for the desorption rates close to the maximum ones are shown in **Fig. 6**. The temperature dependence of the oxygen desorption rate has been calculated without taking the tungsten oxide formation, thus, it is underestimated. The same **Figure** illustrates the temperature dependence of the evaporation rate of molecular oxygen (Al_2O_3 dissociation product) at the surface (curve *3*) calculated as $i^{O_2} = \alpha \cdot 3.5 \cdot 10^{22} (M^{O_2}T)^{-1/2} P_r^{O_2} S$ where α is the molecular condensation coefficient, $\alpha = 1$; $P_r^{O_2}$, the O_2 vapor equilibrium pressure, mm Hg; S, the sapphire sample surface area, cm^2. It is seen that at $T < 1900$ K, the oxygen evaporation rate due to Al_2O_3 dissociation at the sapphire surface, even at $\alpha = 1$, is negligible as compared to its release rate out of the sapphire bulk.

To explain the results obtained and, in particular, the increasing isothermal desorption rates of impurity C and H and matrix oxygen atoms (as CO, O_2, CO_2, H_2, H_2O) out of sapphire, as well as high oxygen desorption rate, especially at low temperatures, a model mechanism is proposed assuming a source of $2V^i$–M^i complex formation. Such a complex is a dumb-bell shaped set including two vacancies, one of which containing an ion while another is free (neutral). The binding energy of ions included in the complex with other ions of

the crystal lattice is lowered due to polarization of the medium surrounding the free vacancy. This increases the probability of the ion-covalent binding breakdown and the resulting formation of atoms that are displaced into the neighboring free neutral vacancies where the ion-covalent binding is recovered after the time interval $\tau = 1/k_1^i$. The subsequent displacement of the atom occurs when other neutral vacancy approaches it. This process (repeating in time) is considered as formation and diffusion of the complexes. According to the model proposed, it is just the impurity C and H atoms and matrix oxygen and aluminum ones that are released out of the sapphire bulk. Note that the matrix Al atoms were not registered due to their condensation at the measuring chamber surface. Therefore, the matrix oxygen and aluminum atoms are assumed to be released in the stoichiometric ratio. This is confirmed by the fact that the sapphire remains stoichiometric under isothermal high vacuum exposure at $T \le T_m$. The rates of ion-covalent binding breakdown ($2V^i$–M^i complex formation) are defined by the following equations: for the matrix oxygen and aluminum atoms

$$q_V^O = C^O \cdot C_V^a k_1^a, \tag{3}$$
$$q_V^{Al} = C^{Al} \cdot C_V^{ct} k_1^{ct},$$

for impurity atoms

$$q_V^i(t) \approx \frac{dC^i(t)}{dt} = \left[C_0^i - C^i(t) \right] C_V^{ct} k_1^{ct}, \tag{4}$$
$$C^i(t) = \frac{1}{V} \int_0^Z \frac{dn^i}{dt}(t) dt,$$

or

$$q_V^i(t) = q_{0V}^i e^{-C_V^{ct} k_1 t}, \tag{5}$$
$$q_{0V}^i = C_0^i C_V^{ct} k_1^{ct},$$

where C_{0V}^i is the initial rate of complex formation; k_1^i, the rate constant of the ion-covalent binding breakdown, s^{-1}; $A_0^i = 10^{14}$ s^{-1}, the frequency pre-exponential factor substantially independent of T; ε_1^i, the ion-covalent binding breakdown energy [6]; C^O, C^{Al}, concentrations of matrix oxygen and aluminum atoms in sapphire, cm^{-3}; C_0^i, initial concentration of impurity atoms, cm^{-3}; $C^i(t)$, the decrease of impurity atom concentration due to desorption, cm^{-3}; C_V^a, C_V^{ct},

concentrations of anionic and cationic vacancies, respectively, arbitrary units; dn^i/dt, desorption rate of impurity atoms as CO, CO$_2$, H$_2$, etc., s^{-1}; V, the sapphire sample volume, cm^3. Note that, as is found, the sapphire crystals grown in high vacuum are stoichiometric and no other phase particles are formed. Thus, in this case, the ratio of released impurity and matrix aluminum atoms to oxygen atoms released as CO, CO$_2$, O$_2$, H$_2$O, O is equal to 2/3.

When the source of $2V^i$–M^i complex formation acts continuously in sapphire, the diffusion and subsequent desorption of atoms and molecules is described for spherical samples as

$$\frac{\partial C_d^i(r,t)}{\partial t} = D^i \frac{1}{r^2} \frac{\partial}{\partial r} \left[\frac{1}{r^2} \frac{\partial C_d^i(r,t)}{\partial r} \right] + q_V^i \tag{6}$$

with boundary conditions

$$C_d^i(r,t) = 0, \quad t = 0, \tag{7}$$

$$\frac{\partial C_d^i(r,t)}{\partial r} = 0, \quad r = 0, \tag{8}$$

for desorption of molecules

$$\frac{\delta \partial C_d^i(r,t)}{\partial t} = \tag{9}$$
$$= -\delta \theta^O(t) C_d^i(r,t) k_d^i - D^i \frac{\partial C_d^i(r,t)}{\partial r}, \quad r = R,$$

for desorption of atoms

$$\frac{\delta \partial C_d^i(r,t)}{\partial t} = -\delta C_d^i(r,t) k_d^i - D^i \frac{\partial C_d^i(r,t)}{\partial r}, \quad r = R,$$

where $\theta^O(t) = C^O(R,t)/C^O$, $C^O(R,t)$ being concentration of oxygen atoms at the surface, cm^{-3}; $\theta^O(t)$, the fraction of active sites at the sapphire surface occupied by oxygen atoms released out of the bulk; δ, the path length of an atom jumping from the occupied vacancy to the neighboring free one, cm; k_d^i, the rate constant of recombinational desorption of particles, s^{-1}.

Solving the diffusion equation by Fourier method, we obtain the distribution of impurity atoms in the complexes:

$$C_d^i(r,t) = \frac{2R^2 q_{0V}^i e^{-C_V^i k_1 t}}{D^i} \sum_{n=1}^{\infty} \frac{\sin\mu_n \cos\mu_n\left(\frac{r}{R}\right)}{\mu_n^3} \times \tag{10}$$
$$\times \left(1 - e^{-\frac{\mu_n^2 D^i}{R^2} t} \right),$$

and the distribution of impurity atoms included in the complexes:

$$C_d^O(r,t) = \frac{2R^2 q_V^O}{D^O} \sum_{n=1}^{\infty} \frac{\sin\mu_n}{\mu_n^3} \cos\mu_n \frac{r}{R} \times \quad (11)$$

$$\times \left(1 - e^{-\frac{\mu_n^2 D^O}{R^2} t} \right),$$

where μ_n are the roots of characteristic equation $\operatorname{ctg}\mu_n = \mu_n / B_i$, $B_i = \delta\theta^O(t)Rk_d / D^i$ derived from the boundary condition (9).

Restricting ourselves to the first item of the sum of Eqs.(10), (11), we can reduce the equation for the diffusion rate of impurity and matrix oxygen and aluminum atoms out of the sapphire bulk to the form

$$\frac{dn^i}{dt} = \frac{2Rq_{OV}^i e^{-C_V^i k_1 t} \sin^2\mu_1}{\mu_1^2} \left[1 - e^{-\frac{\mu_1^2 D^i}{R^2} t} \right], \quad (12)$$

$$\frac{dn^i}{dt} = \frac{2Rq_V^i \sin^2\mu_1}{\mu_1^2} \left[1 - e^{-\frac{\mu_1^2 D^i}{R^2} t} \right]. \quad (13)$$

The equation for the recombinational desorption of molecules takes the form

$$\frac{dn^i}{dt} = \delta\theta^O k_d^i \frac{2R^2 q_{OV}^i e^{-C_V^i k_1^i t} \sin\mu_1 \cos\mu_1}{\mu_1^3 D^i} \times \quad (14)$$

$$\times \left[1 - e^{-\frac{\mu_1^2 D^i}{R^2} t} \right] - \alpha v^i(t),$$

where
$v^i(t) = 3.5 \cdot 10^{22} (M^i T)^{1/2} P^i(t),$

$P^i(t) = P_0^i [1 - e^{-\frac{\mu_1^2 D t}{R^2}}] e^{-C_V^{ct} k_1^{ct} t}$ is the pressure of gas (CO) released out of sapphire.

For desorption of matrix atoms, we get

$$\frac{dn^i}{dt} = \delta k_d^i \frac{2q_V^i R^2 \sin\mu_1 \cos\mu_1}{D^i \mu_1^3} \times \quad (15)$$

$$\times \left[1 - e^{-\frac{\mu_1^2 D^i}{R^2} t} \right] - \alpha v^i(t),$$

where
$v^i(t) = 3.5 \cdot 10^{22} (M^i T)^{1/2} P^i(t),$

$P^i(t) = P_0^i \left(1 - e^{-\frac{\mu_1^2 D^i t}{R^2}} \right).$

The same equations describe the diffusion and desorption of gases out of sapphire single-crystalline plates. In this case, the plate half-thickness h is to be substituted for R.

Note that the impurity and matrix atoms from the gas phase may be re-dissolved in sapphire only if those are released in a non-stoichiometric ratio, that is, if there is an excess concentration of cationic or anionic vacancies forming traps for the atoms being dissolved.

The CO desorption at $T = 1380$ K was analyzed for the section 1 of curve 3, that is, at $t = t_1$, where the effect of sapphire surface contamination with carbon is negligible, $\frac{dn^{CO}}{dt} = \max$, $\theta^O = \max$, $\mu_1 = const$. Since in high vacuum $v^i(t) = 0$, then, differentiating Eqs.(14) and (15) with respect to t at $t = t_1$, we obtain for desorption of impurity and matrix atoms

$$\frac{\frac{d}{dt}\left(\frac{dn^i}{dt}\right)}{\frac{dn^i}{dt}} = \quad (16)$$

$$= \frac{\mu_1^2 D^i}{R^2} \left[\frac{e^{-\frac{\mu_1^2 D^i}{R^2} t_1} - e^{-\frac{\mu_1^2 D^i}{R^2} t_m}}{1 - e^{-\frac{\mu_1^2 D^i}{R^2} t_1}} \right],$$

$$\frac{\frac{d}{dt}\left(\frac{dn^i}{dt}\right)}{\frac{dn^i}{dt}} = \frac{\mu_1^2 D^i}{R^2} \frac{e^{-\frac{\mu_1^2 D^i}{R^2} t_1}}{1 - e^{-\frac{\mu_1^2 D^i}{R^2} t_1}}. \quad (17)$$

Differentiating the experimental curve 1 (Fig. 3) with respect to t using the graphic technique at $t_1 = 4.8 \cdot 10^3$ s, we obtain

$$\frac{\frac{d}{dt}\left(\frac{dn^{CO}}{dt}\right)}{\frac{dn^{CO}}{dt}} = 6.4 \cdot 10^{-5} s^{-1}. \quad (18)$$

From Eq.(4), we get

$$C_V^{ct} k_1^{ct} = \frac{1}{t} \ln \frac{C_0^C}{C_0^C - C^C(t)}, \quad (19)$$

$$C^C(t) = \frac{1}{V} \int_0^t \frac{dn^{CO}}{dt} dt,$$

where $\frac{dn^{CO}}{dt}$ is the experimental desorption rate, s^{-1}. $C^C(t)$ is found by graphic integration of the area under curve of $\frac{dn^{CO}}{dt}$ (Fig. 3) for $T = 1380$ K, $0 < t \le 4.8 \cdot 10^3$ s. Substituting the experimental $C^C(t)$ value into (19), we get

$$C_V^{ct} k_1 = 4.5 \cdot 10^{-6} s^{-1}. \quad (20)$$

Using (20), we derive from (16)

$$\frac{\mu_1^2 D^C}{R^2} = 4 \cdot 10^{-4} s^{-1}. \qquad (21)$$

Using the extreme condition $\frac{d}{dt}\left(\frac{dn^{CO}}{dt}\right) = 0$, we obtain the formula to calculate the time of maximum CO desorption rate:

$$t_m = \frac{R^2}{\mu_1^2 D^C} \ln\frac{\mu_1^2 D^C}{R^2 C_V^{ct} k_1^{ct} t}. \qquad (22)$$

Differentiating graphically the experimental curve of molecular oxygen desorption rate with respect to t at $t = 4.8 \cdot 10^3$ s, we find

$$\frac{\frac{d}{dt}\left(\frac{dn^{O_2}}{dt}\right)}{\frac{dn^{O_2}}{dt}} = 8.2 \cdot 10^{-5} s^{-1} \qquad (23)$$

and then, substituting (23) into (17), we obtain

$$\frac{\mu_1^2 D^O}{R^2} = 3.5 \cdot 10^{-4} s^{-1}. \qquad (24)$$

Using (20) and experimental value of $[C_0^C - C^C(t)]$, we obtain from (4) $q_V^C = 1.06 \cdot 10^{14}$ cm^{-3}/s, and then, substituting (20), (21), and [q_V^C into (12), we find $\mu_1 = 1.89$ (54.17°). Substituting μ_1 into (21), (24), we obtain DC = $4.5 \cdot 10^{-6}$ cm2/s, DO = $3.9 \cdot 10^{-6}$ cm2/s. An atom in sapphire crystal lattice has two jump paths, i.e., from the vacancy occupied by it to the adjacent free one and vice versa. Therefore, the pre-exponential factor in the formula for diffusion coefficient is calculated using the formula $D_0 = \delta^2/2\tau_0$, $\tau_0 = h/k_B T$, where τ_0 is the thermal vibration period of the atoms in crystal lattice. Using the calculated D_0, D^C, D^O, we find the diffusion activation energy for the atoms and vacancies: $\varepsilon_m^C = 21434$ cal/mol, $\varepsilon_m^O = 21826$ cal/mol, and then the diffusion coefficients for other temperatures can be calculated. Note that the desorption rates and $C_V k_1$ values can be calculated after each temperature jump (Figs. 3, 4) using (14), (19) for $0 \leq t \leq \Delta t_1$ (Δt_1 being desorption time intervals at temperature T_i, $i = 1, 2, 3...$), if the carbon atoms released prior to the temperature jump are subtracted from the initial carbon atomic concentration C_0^C.

Table 1.

T, K	$C_V k_1$
1370	$4.55 \cdot 10^{-6}$
1650	$1.1 \cdot 10^{-5}$
1700	$1.6 \cdot 10^{-5}$
1990	$4.3 \cdot 10^{-5}$
2120	$7.7 \cdot 10^{-5}$
2250	$1.0 \cdot 10^{-4}$
2327	$1.2 \cdot 10^{-4}$

Correspondingly, using experimental data of Figs. 3, 4, we find, using formula (19), the $C_V k_1$ values presented in Table 1. Using the found diffusion and desorption parameters for carbon atoms in the form of CO, the time t required to remove carbon from the raw material used to grow sapphire single crystals. Since it is just CO being released at the crystal/melt phase interface that is the main source of gas bubble formation, then, the gas micropore formation can be excluded completely or reduced substantially by purification of raw material from carbon.

As noted above, the desorption of impurity and matrix atoms out of sapphire in high vacuum does not cause any deviation from sapphire stoichiometry. It follows therefrom that cations (impurity atoms plus aluminum ones) and anions (oxygen atoms) are released out of sapphire in practically stoichiometric ratio. In this connection, the total formation rates q_V^{Al}, q_V^O of cationic and anionic complexes ($2V^{ct}$–Al, $2V^a$–O) that define the desorption of matrix O and Al atoms and impurity ones in the form of CO and CO$_2$ can be calculated as

$$q_V^{Al} = \frac{C^{Al}}{C^C} q_V^C, \quad q_V^O = 1.5 \cdot q_V^{Al}, \qquad (25)$$

where $C^{Al} = 9.4 \cdot 10^{21}$ cm^{-3}, $C^C = 2.4 \cdot 10^{19}$ cm^{-3}.

Note that Al, O, C and other atoms are released out of sapphire also due to decomposition of Al$_4$O$_4$C and Al$_4$C$_3$ inclusions present in sapphire. That process, however, cannot be considered separately, since Al and O atoms included in aluminum oxycarbides and carbides lose their belonging thereto after the first jump into free vacancy. Then those become indistinguishable from other impurity and matrix atoms being in substitution positions.

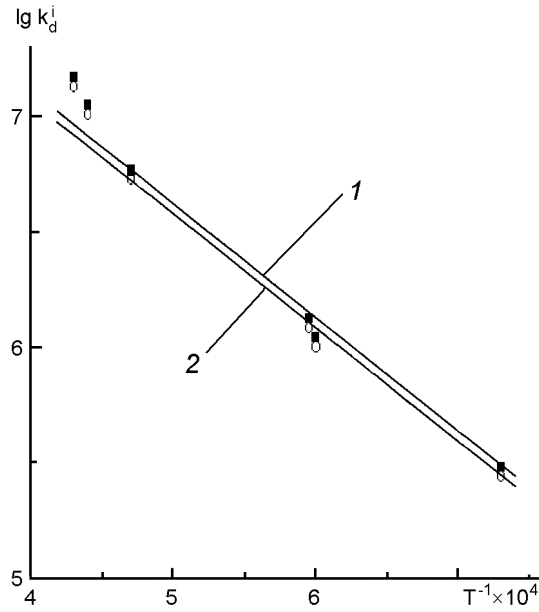The experimental data on CO, CO$_2$ and O$_2$ desorption (Figs. 3, 4) and the calculated

Fig. 7. Temperature dependences of desorption rate constant for for CO (*1*) and O_2 (*2*). $\varepsilon_d^{CO} = 22750$ cal/mol.

diffusion parameters make it possible to determine the recombinational desorption rate constants of the gases. To that end, using the continuity condition for flow of atoms from the sapphire bulk to its surface and from the surface to vacuum in the form of molecules, we obtain:

for CO desorption at $t = t_m$

$$k_d^{CO} = \frac{D^C D^O N^O \mu_1^4}{2\delta R^3 q_V^O \cos^2\mu_1}. \qquad (26)$$

For O_2 desorption at $t >> R^2/\mu_1^2 D^O$

$$k_d^{O_2} = \frac{(D^O)^2 N^O \mu_1^4}{2\delta R^3 q_V^O \cos^2\mu_1}. \qquad (27)$$

For desorption of matrix atoms

$$k_d^i = \frac{D^i}{\delta R}\mu_1 \mathrm{tg}\mu_1. \qquad (28)$$

Fig. 7 presents the $\lg k_d^i(1/T)$ dependences calculated as

$$\lg k_d^i = \lg A - \varepsilon_d^i/4.55 \cdot T, \qquad (29)$$

(*A* being the pre-exponent in the Arrhenius equation). It is seen that at $T \leq 2100$ K, the experimental points fit rather well the straight lines, the diffusion activation energy values for CO and O_2 being approximately the same. The temperature dependences of isothermal desorption rate constants for Al and O atoms (cations
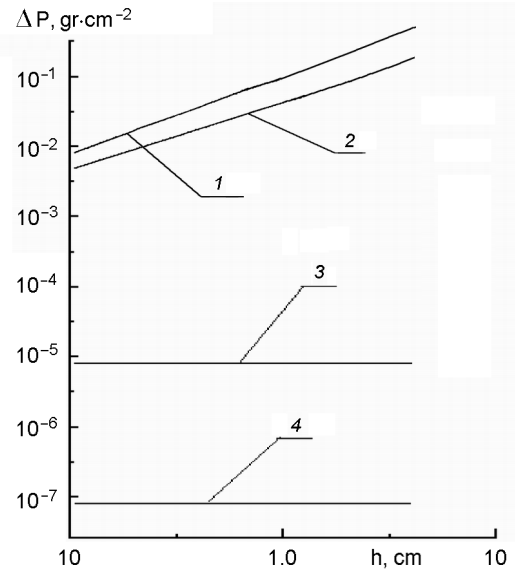

Fig. 8. Dependence of released oxygen and aluminum mass on the sapphire sample thickness. Release of Al and O atoms at $T = 2300$ K (*1*) and 2000 K (*2*); evaporation of Al_2O_3 dissociation products at the surface at $T = 2300$ K (*3*) and 2000 K, gr.cm^{-2} (*4*). $t = 3.6 \cdot 10^3$ s.

and anions) calculated using (28) are presented in Table 2. These constants are seen to be essentially the same for Al and O atoms released out of the bulk and θ^O to be less than recombinational desorption rate constants for CO and O_2 molecules.

According to the mechanism proposed, dn^i/dt depends on the sapphire block radius (or thickness). Fig. 8 shows the mass loss of a flat sapphire sample per 1 h due to release of matrix atoms out of its bulk as a function of *h*. The mass loss has been calculated assuming $D^{Al} = D^O$ using the formula

$$\Delta P \approx \frac{2h\sin^2\mu_1}{\mu_1^2 N_A}\left(q_V^{Al} \cdot A^{Al} + q_V^O \cdot A^O\right) \times \qquad (30)$$
$$\times \left[t - \frac{h^2}{\mu_1^2 D}\left(1 - e^{-\frac{\mu_1^2 D}{h^2}t}\right)\right],$$

where N_A is Avogadro number; A^{Al}, A^O, atomic masses of Al and O. It is well seen that ΔP increases with the increase of h_0. The same Figure (curves 3, 4) shows the sapphire mass losses due to evaporation of Al_2O_3 dissociation products from the surface. Comparing the curves, it can be seen that at $T \leq 2300$ K, the latter contribution to the mass loss can be neglected. The experimental studies of $\Delta P(h)$ seem to be us-

Table 2.

T, K	k_d^{Al}, s^{-1}	k_d^{O}, s^{-1}
1370	$1.7 \cdot 10^3$	$1.5 \cdot 10^3$
1650	$7.3 \cdot 10^3$	$6.5 \cdot 10^3$
1700	$9.2 \cdot 10^3$	$8.4 \cdot 10^3$
1990	$2.7 \cdot 10^4$	$2.4 \cdot 10^4$
2120	$3.8 \cdot 10^4$	$3.7 \cdot 10^4$
2250	$5.7 \cdot 10^4$	$5.3 \cdot 10^4$
2327	$6.9 \cdot 10^4$	$6.5 \cdot 10^4$
ε^i, cal/mol	≈ 23625	$\approx Б№$

Fig. 9. Temperature dependences concentration of neutral cationic (*1*) and anionic (*2*) vacancies.

able to check the proposed model of O and Al atoms release out of sapphire bulk.

According to the model, the gas-vacancy complexes are formed in sapphire due to breakdown of ion-covalent bindings that are weakened due to polarization of the medium around the vacancies. If $k_1 = Ae^{-\varepsilon_1/kT}$, $C_V = e^{-\varepsilon_W/kT}$, then the complex formation rates q_V^i should depend on temperature exponentially, too. Really, it is no the case. In this connection, let the effect of concentration and state of vacancies on the gas-vacancy complexes formation rate be considered. The dependence $C_V^i(T)$ calculated using (3) under assumption $k_1 = 10^{14}e^{-\varepsilon_1/kT}$, $\varepsilon_1 = 61,000$ cal/mol [6] is shown in Fig. 9. It is seen that the concentrations of both cationic and anionic vacancies do not increase but decrease at the temperature elevation. Such a dependence can be explained assuming that the diffusion of atoms occurs in neutral vacancies, the concentration of the latter drops due to ionization as temperature increases.

To check if the proposed isothermal desorption model of impurity and matrix atoms corresponds to experimental data, the calculated $(dn^i/dt)(t)$ curves have been plotted. As an example, Fig. 3 presents the calculated curve 1a for CO desorption at $T = 1380$ K. Similarly, in Fig. 6, the curve *4* shows the calculated temperature dependence of maximum CO desorption rate. Both those curves coincide with experimental ones. Thus, the model mentioned describes well the experimental results obtained at $1380 < T < 2100$ K.

C, O and H atoms diffusing out of the crystal and melt are released at the crystal/melt interface, too. At the melt concentration overcooling due to recombination of atoms and side diffusion, the formed CO, CO_2, H_2 and O_2 molecules are accumulated in intercellular hollows. Depending on size
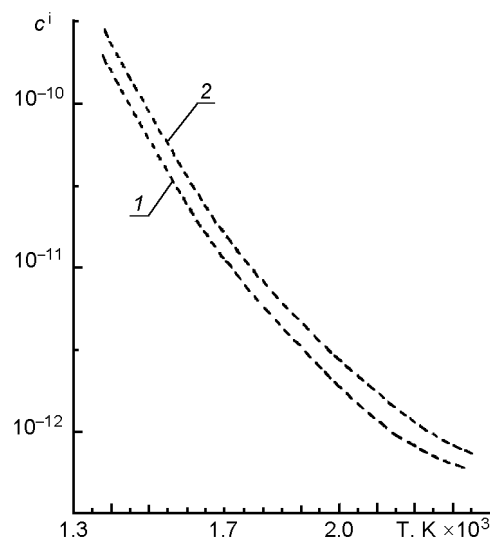
of the hollow and the gas accumulation, isomeric equilibrium bubbles of 10^{-3} to 10^{-2} cm in diameter and non-isomeric pores are formed [1–3]. In the bubbles included in the crystal the CO_2 and O_2 molecules are subjected to dissociation (the dissociation energy values in brackets): $CO_2 = CO + O$ ($\varepsilon_{dis}^{CO_2} = 156000$ cal/mol), $O_2 = 2O$ ($\varepsilon_{dis}^{O_2} = 117000$ cal/mol). CO does not dissociate essentially ($\varepsilon_{dis}^{CO} = 256000$ cal/mol). That is why only CO and H_2 are revealed in the bubbles [4, 5]. Sapphire grown in a high vacuum is essentially stoichiometric, no other phase particles being formed therein. The low excess concentration of oxygen vacancies therein (about 10^{16} cm^{-3}) seems to be defined by impurity atoms being in the substitution positions and having other valence than Al ones.

However, as the excess oxygen vacancies are present in sapphire maily as F color centers, the sapphire non-stoichiometry is thermodynamically equilibrium. The second phase deposition at the expense of excess Al atoms in the thermodynamically equilibrium non-stoichiometric sapphire is impossible, that is confirmed in experiment. The second phase particles being found most often in the near-bottom sapphire layer seem to deposit at the crystal/melt interface, perhaps due to formation of compounds comprising Al_2O_3 and impurity oxides and accumulated in the near-bottom melt layer, possibly due to thermal diffusion [7], ortermal convection of the melt.

To conclude, isothermal desorption of impurity and matrix atoms (as CO, CO_2, O_2, H_2, H_2O) out of sapphire has been studied in ex-

periment and theoretically. It has been shown that as the sapphire temperature is increased stepwise, the isothermal desorption rates of impurity atoms in the form of CO, CO_2, H_2, H_2O increase first in time up to certain maximum values and then decrease. The desorption rate of matrix oxygen atoms does not attain a maximum in time. As the temperature is increased, the time required to attain the maximum desorption rate is shortened. A theoretical model has been proposed for diffusion mechanism of the atoms included in gas-vacancy complexes $2V^i$–M^i (M^i being an atom, V^i, a neutral vacancy). According to the model, the gas-vacancy complexes are formed due to breaking of ion-covalent (polarization) bonds in sapphire. The impurity and matrix atoms that are diffused to the surface as components of the complexes are transformed into adsorbed state, then a fraction thereof becomes desorbed while another one becomes recombined into molecules and then desorbed. The equations describing the diffusion and desorption have been derived. Considering the experimental results on the isothermal desorption and using the equations obtained, the kinetic diffusion parameters for atoms (vacancies), the desorption rate constants for CO, CO_2, O_2, have been determined and the activation energy values for those processes have been esti-mated. For thin sapphire samples, the release rates of cations (Al, C, H, etc.) and anions (oxygen atoms) out of bulk are in proportion to the sample thickness and exceed considerably the corresponding evaporation rates at Al_2O_3 dissociation at the surface.

References

1. N.P.Katrich, Yu.A.Borodenko, E.P.Solovyova, V.E.Kachala, in: Single Crystals and Engineering, 11th Issue, VNIIM Publ., Kharkov (1975), p.20 [in Russian].

2. N.P.Katrich, V.E.Kachala, A.Ya.Dan'ko et al., in: Gas Porosity Formation in Corundum, Tungsten, and Molybdenum: A Review. CNII Atominform, Moscow (1987), p.27 [in Russian].

3. A.T.Budnikov, A.E.Vorobyov, V.N.Kanischev et al., Preprint №4, VNIIM Publ., Kharkov (1990) [in Russian].

4. A.E.Vorobyov, N.P.Katrich, Yu.P.Miroshnikov, in: Republ. Interdepartmental Coll. of Sci. Commun., 22th Issue, Naukova Dumka, Kiev (1989), p.32 [in Russian].

5. N.P.Katrich, E.M.Khizhnyak, in: Single Crystals and Engineering, 12th Issue, VNIIM Publ., Kharkov (1976), pp. 26, 33 [in Russian].

6. E.P.Elutin, Yu.A.Pavlov, V.P.Polyakov, Interaction of Metal Oxides with Carbon, Metallurgia, Moscow (1976) [in Russian].

7. P. Shyumon, Diffusion in Solids , Metallurgia, Moscow (1966), [in Russian].

Дифузія та подальша ізотермічна десорбція домішкових та матричних атомів з сапфіру та його розплаву

М.П.Катрич, О.Т.Будников, С.І.Кривоногов, Ю.П.Мірошников

Досліджено ізотермічну десорбцію домішкових та матричних атомів з об'єму сапфіру у складі CO, CO_2, H_2, H_2O. Запропоновано теоретичну модель механізму дифузії атомів у сапфірі у складі газо-вакансійних комплексів $2V^i$–M^i (M^i — атом, V^i — нейтральна вакансія). Згідно з моделлю, газо-вакансійні комплекси утворюються внаслідок розриву іонно-ковалентних зв'язків у сапфірі. Домішкові та матричні атоми, продифундувавши до поверхні у складі комплексів, переходять в адсорбований стан, після чого одна частка їх десорбується, а інша рекомбінує у молекули, а потім десорбується. Одержано рівняння, що описують дифузію та десорбцію, визначено параметри дифузії та десорбції атомів та молекул.